An Orthogonal Click-Chemistry Approach to Design Poly(glycerol monomethacrylate)-based Nanomaterials for Controlled Immunostimulation

Lakshminarayanan Ragupathy, Douglas G. Millar, Nicola Tirelli, Francesco Cellesi*

L. Ragupathy,[+++] F. Cellesi[+]
School of Pharmacy and Pharmaceutical Sciences, University of Manchester, Oxford Road, Manchester M13 9PT, UK
D. G. Millar[++]
Faculty of Life Sciences, University of Manchester, M13 9PT, United Kingdom
N. Tirelli
School of Biomedicine and School of Materials, University of Manchester, Laboratory for Polymers and Biomaterials, Stopford Building, Manchester M13 9PT, UK
[+]Present address: 1. Fondazione CEN - European Centre for Nanomedicine, Piazza Leonardo da Vinci 32, 20133 Milan, Italy; 2. Fondazione IRCCS Ca' Granda Ospedale Maggiore Policlinico, Via Pace 9, I-20122 Milan, Italy; 3. Dipartimento di Chimica, Materiali ed Ingegneria Chimica "G. Natta". Politecnico di Milano, Via Mancinelli 7, 20131 Milan, Italy
E-mail: francesco.cellesi@polimi.it
[++]Present address: Campbell Family Institute for Breast Cancer Research, Princess Margaret Cancer Centre, 620 University Avenue, Toronto, Ontario, Canada M5G 2C1
[+++] Present address: Corporate Research and Development Center, HLL Lifecare Limited (A Government of India Enterprise), Akkulam, Sreekaryam, Trivandrum 695017, India

1. Introduction

The use of synthetic functional polymers has received considerable attention in nanomedicine, mainly due to the possibility to tailor their physicochemical properties and bioactivity according to the specific requirements of a biomedical application.[1] Synthetic polymers dispersed in aqueous suspension, in form of micelles, dendrimers, nanoparticles, have shown great potential as drug and gene delivery systems.[1,2] Generally, these materials are designed to evade the immune system, i.e., their administration is supposed not to provoke defensive and potentially dangerous immune responses.[3] However, there is an increasing number of examples of polymeric materials designed to stimulate and/or modulate immune responses.[4] A variety of systems, including water-soluble polymers and polymer-based nanoparticles, have been used as synthetic vaccines, in order to deliver specific antigens to antigen-presenting cells (APC), such as dendritic cells (DC) and macrophages, and to control the final presentation of the antigenic groups to targeted T cells.[5–7] In this way, advanced polymeric materials have shown promise as new prophylactic vaccines for infectious diseases,[6,8] as well as new immunotherapeutics for cancer, allergies, and autoimmune diseases.[6] Biomaterials can also be used as adjuvants, i.e., they stimulate the immune system by activating APCs through specific receptor mediated signaling,[9] with the goal of influencing the way antigens are recognized by immune cells and interpreted as danger signals. To date, however, only aluminium salts[10] (alum, which precipitates the antigen at the site of administration for a more efficient uptake by peripheral APCs) are the sole adjuvants approved for human use in the majority of countries worldwide. Although alum is able to induce a good antibody (Th2) response, it has little capacity to stimulate cellular (Th1) immune response, which is essential for protection against several pathogens.[10] Moreover, alum may cause local and systemic side-effects (including sterile abscesses, eosinophilia and myofascitis),[10] and raised concerns regarding the possible role of aluminium accumulation in neurodegenerative diseases.[11] Consequently, there is a major unmet need for safer and more effective immunoactive materials, and although several natural and synthetic compounds (e.g., lipopolysaccharides, CpG DNA and other toll-like-receptor targeting substances)[12,13] have been investigated for adjuvant activity, their toxicity and uncontrolled immunogenicity have hindered their use in humans.[10]

In order to overcome current limitations in vaccine and adjuvant technology, we have proposed a simple, versatile and robust synthetic route for the preparation of novel functional polymeric materials designed to achieve a controlled immunostimulation, without causing strong immune reaction. These biocompatible polymers are capable of coupling a variety of different bioactive moieties, including ligands for specific cell targeting and activation, immunomodulators, and antigenic peptides. The tuneable conjugation of these active components may allow to identify the key parameters and the optimal system for specific vaccine therapies. In this work, we have investigated a new platform of immune active polymers based on poly(glycerol monomethacrylate) (PGMMA); the latter is a synthetic hydrophilic polymer which has showed promising characteristics for biomedical applications.[14–18] PGMMA can be easily synthesized under controlled/living polymerisation conditions via Atom Transfer Radical Polymerisation (ATRP),[19,20] and presents low toxicity,[16] substantial absence of interactions with proteins,[14,15] and reduces cell adhesion on surfaces.[17] In comparison with other ''stealth'' synthetic polymers, PGMMA offers the advantage of a high density of functional groups. The two -OH groups per monomeric unit, while providing high hydrophilicity, can be easily derivatised to obtain, for instance, drug-conjugated materials.[21]

The synthesis of PGMMAs was carried out via ATRP starting from an alkyne-functionalized initiator (propargyl 2-bromoisobutyrate). Following an orthogonal click chemistry approach, the resulting propargyl-terminated PGMMAs were further modified with dangling acrylate groups at different degree of functionalisation, by simple acrylation of the hydroxyl groups with acryloyl chloride. Acrylates were then able to react quantitatively with thiol-containing moieties (such as thiolated saccharides, eventually cysteine-containing peptides and proteins) through Michael-type addition under mild conditions and at a physiological pH (Scheme 1). In this work we used thiomannose as a thiol, since grafted mannose is expected to activate the complement system in vivo and to be recognised by mannose receptors on APC, which are involved in immune surveillance (pathogen recognition and uptake) and antigen presentation pathways.[22,23] The propargyl terminal group, unaltered during the Michael-type addition, can be then orthogonally modified via Huisgen cycloaddition using azide end-capping groups, and utilized to graft the polymer to any additional 'building blocks', including a fluorophore, a bioactive macromolecule, a nanoparticle, thus increasing the functionality of the biomaterial.

This facile synthetic approach allows the preparation of biocompatible hydrophilic polymers with a full control over molecular weight, functionality, tailorable immunostimulation of APCs, and with the characteristic to expand their functionality and bioactivity through simple ''click'' reactions. In this article, propargyl-terminated PGMMAs of controlled degree of mannosylation were characterised in vitro in terms of cytotoxicity, capability of stimulating cytokine production (TNFα) and surface activation marker (CD40) expression by bone marrow-derived dendritic cells (BMDCs), and cellular uptake.

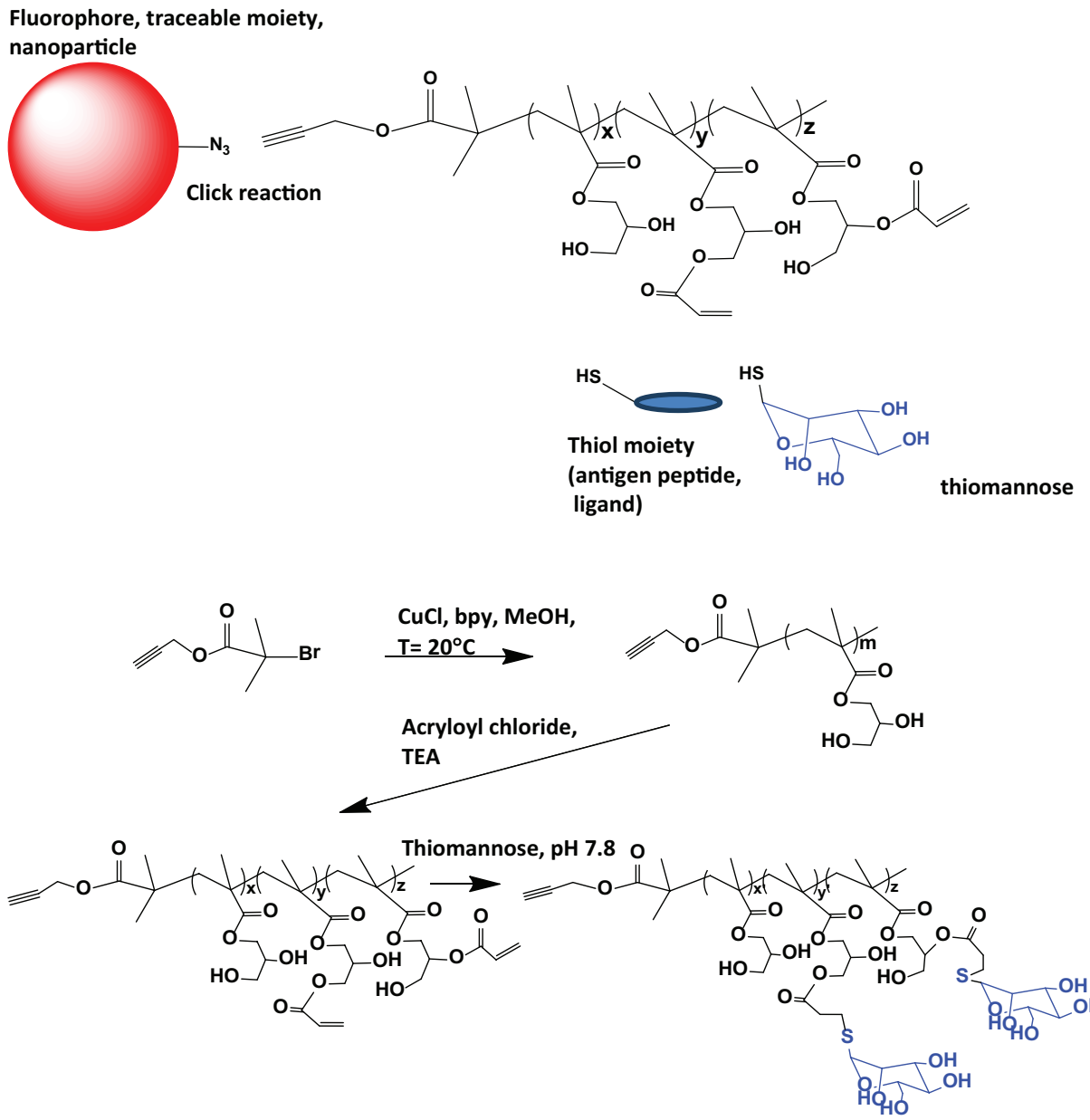

Scheme 1. Propargyl-terminated poly(glycerol methacrylate)s, modified with dangling acrylate groups, can be easily conjugated with thiol-containing molecules (thiolated mannose, cysteine containing peptides) through Michael-type addition. Azide-alkyne Huisgen cycloaddition can be used to prepare a final traceable polymer for in vitro tests or more complex immune active nanomaterials. Propargyl-terminated PGMMAs were synthesized through ATRP in methanol, functionalised with acrylates through esterification and mannosylated through Michael-type addition of thiomannose in physiological pH.

2. Experimental Section

2.1. Materials

Dicyclohexyl carbodiimide, propargyl alcohol, 2-bromoisobutyric acid, 4-dimethylaminopyridine, ethyl 2-bromoisobutyrate, CuCl, CuBr, 2,2'-bipyridine (bpy), dimethylacetamide, 2,6-di-*tert*butyl-4-methylphenol (butylated hydroxytoluene, BHT), acryloyl chloride, triethylamine, α-D-mannose pentaacetate, mannan from *Saccharomyces cerevisiae*; thioacetic acid, $BF_3 \cdot Et_2O$, anhydrous Na_2SO_4, sodium bicarbonate, potassium methoxide, DOWEX 50WX8-200, triphenylphosphine (TPP), 11-azido-3,6,9-trioxaundecan-1-amine (11-ATA) and Azide MegaStokes dye 673 (Azide-MS673), hexamethyl-triethylene tetraamine, NaOD, D_2O, and silica gel 60 Å were purchased from Sigma-Aldrich (Gillingham, UK), as well as methylene chloride, methanol, hexane, ethyl acetate, dimethylformamide (DMF), and tetrahydrofuran. $CDCl_3$, dimethylsulfoxide (DMSO)-d_6, and CD_3OD were bought from Cambridge Isotope

Laboratories, Inc. (Ibstock, UK). 1-Glycerol monomethacrylate (GMMA) was obtained from Cognis Performance Chemicals UK Ltd. (Southampton, UK). Dialysis tubes and phosphate buffer tablets were acquired from Spectrum labs (Breda, NL) and OXOID (Basingstoke, UK), respectively.

All materials were used as received from the supplier. GMMA contained about 2 mol% of 2-glycerol monomethacrylate, which was not separated.

2.2. Molecular Characterisation

2.2.1. Spectroscopy

^{1}H NMR spectra were recorded on 1 wt% polymer solutions in deuterated solvent using a 300 MHz Bruker NMR spectrometer. FT-IR spectra were recorded in Attenuated Total Reflectance (ATR) mode on a Tensor 27 Bruker spectrometer.

2.2.2. Gel Permeation Chromatography (GPC)

Polymer molecular weights and their distribution of the synthesized PGMMAs were determined by GPC in dimethylacetamide and 0.5% $LiNO_3$ using a combination of two 10 μm (30 cm) different columns (PL Gel 500Å, 2MixedB) at 50 °C. The flow rate was maintained at 1.0 mL min^{-1} using a pump Waters 501. Detection was performed with a differential refractometer ERC-7515A. Calibration was done by narrowly distributed poly(ethylene glycol) standards.

2.3. Synthesis of the ATRP Initiator Propargyl 2-Bromoisobutyrate (PgBiB)

The propargyl ATRP initiator PgBiB was synthesized as reported in literature.[24] Propargyl alcohol (4.27 mL, 0.076 mol) and 2-bromoisobutyric acid (12.13 g, 0.073 mol) were dissolved in 50 mL of methylene chloride and cooled down at 0 °C in an ice-water bath. Dicyclohexyl carbodiimide (15.0 g, 0.073 mol) was dissolved in 20 mL methylene chloride and slowly added into the reaction mixture while stirring. A solution of 4-dimethylaminopyridine (0.5 g) in 20 mL methylene chloride was then added over a period of 5 min. The reaction flask was kept at 0 °C for 1 h and then left at room temperature for 24 h under stirring. The mixture was filtered to remove the precipitated dicylohexylurea, concentrated by a rotary evaporator, and the final product was distilled under vacuum. Yield: 63%; ^{1}H NMR ($CDCl_3$): $\delta = 4.77$ (d, $J = 2.4$ Hz, 2H, -CH_2–OCO-), 2.51 (t, $J = 2.4$ Hz, 1H, CH≡C-), 1.96 (s, 6H, -OCO–$(CH_3)_2$–Br). FT-IR (ν): 3290 (C≡C–H), 2100 (-C≡C-), 1740 cm^{-1} [-(C = O)–O].

2.4. ATRP of GMMA

A mixture of PgBiB or alternatively ethyl 2-bromoisobutyrate (EBiB) (1.2/0.6/0.3 mmol; 247/123/62 mg; target degree of polymerisation (DP) = 25/50/100) and GMMA (4.825 g, 30 mmol), was added to a 50 mL vessel of a Carousel parallel reactor (from Radleys, UK). The mixture was degassed by purging the flask with nitrogen gas for 30 min. Nitrogen-degassed methanol (HPLC grade; 5.0 mL) was then added to the flask using a nitrogen-purged syringe, and the solution was purged for an additional 5 min. The copper catalyst (Cu(I)Cl; 1.2/0.6/0.3 mmol; 120/59/30 mg) and bpy ligand (2.4/1.2/0.6 mmol; 375/187/94 mg) were quickly added to the flask, while maintaining a slow nitrogen purge. The reaction mixture was magnetically stirred for 4 h at 20 °C. Each polymerization was terminated by dilution with aerated methanol. The reaction solution turned from brown to blue-green, indicating aerial oxidation of the Cu(I) to Cu(II). This solution was then passed through a silica gel column to remove the copper catalyst, resulting in a colourless solution. The solvent was removed under reduced pressure at 30 °C to give an off-white solid and a ^{1}H NMR spectrum was recorded in CD_3OD to determine the monomer conversion. Crude PGMMA was re-dissolved in methanol (HPLC grade) and then precipitated in THF (HPLC grade); this dissolution/precipitation cycle was then repeated. The purified polymer was dried under vacuum and ^{1}H NMR spectra were recorded in CD_3OD in order to assess its purity. Molar masses of PGMMA synthesized from PgBiB (Pg-PGMMA) were also estimated by ^{1}H NMR (see Supporting Information).

Yield: 74%; ^{1}H NMR (CD_3OD): $\delta = 0.7$–1.4 (broad, 3H –$CH_2C(CH_3)$– in main chain), 1.5–2.3 (broad, 2H, –$CH_2C(CH_3)$–in main chain), 3.4–4.4 (broad, 5H, –OCH_2CH(OH)CH_2(OH)). FT-IR (film on ATR crystal): 3648–3080 (ν OH), 2953 (ν_{as} CH), 2888 (ν_s CH), 1715 (ν C=O ester), 1457 (d 1457 (δ O–CH_2), 1395, 1322, 1245, 1151 (ν C–O–C), 928, 859, 662 cm^{-1}.

2.5. Kinetic Investigation of ATRP of GMMA

ATRP of GMMA was performed with PgBiB and EBiB using the experimental conditions as described above. A 250 μL sample was withdrawn from the reaction mixture during the course of the reaction (at 0.17, 0.5, 1, 2, 3, and 4 h) and analyzed by ^{1}H NMR spectroscopy using D_2O as solvent. The concentrations of the reactants (monomer vinyl signals $CH_2 = C(CH_3)$- at $\delta = 5.5$ and 6.0 ppm) compared to the product ($\delta = 0.7$–1.4, –$CH_2C(CH_3)$–in main chain) were calculated with respect to reaction time by ^{1}H NMR analysis.

2.6. Acrylation of PGMMA

Acrylated Pg-PGMMAs – target degree of acrylation 10, 20 and 40 mol% acrylate per monomeric unit – were obtained by dissolving 300 mg of Pg-PGMMA-25 (ca. 3.6 mmol of –OH), 53/113/174 mg (0.5/1.15/1.7 mmol) triethylamine, 3/6/10 mg (0.01/0.03/0.04 mmol) of BHT in 5 mL DMF. Acryloyl chloride (33/70/108 mg, 0.26/0.56/0.86 mmol) was slowly added to the above reaction mixture at ice cold temperature, and kept under stirring overnight at room temperature. Then, 25 mL of purified water was added to the reaction mixture and the product was purified by dialysis using standard regenerated cellulose tubes, molecular weight cut-off (MWCO) = 1 kDa, for 3 d, and isolated by freeze drying. Yield: 62%.

^{1}H NMR (DMSO-d_6) of the obtained product was examined and the peaks corresponding to $CH_2 = CH$–COO- protons ($\delta = 5.8$–6.6 ppm) were compared to the CH_3 protons of the main polymer chain ($\delta = 0.80$–1.20 ppm, –$CH_2C(CH_3)$–) to calculate the degree of acrylation (values calculated for the three polymers: –CH_2-$C(CH_3)$, 13, 25 and 42 mol% acrylate/mol monomeric unit).

2.7. Synthesis of 1-Thio-α-D-mannopyranose

2.7.1. Synthesis of 1-*S*-Acetyl-2,3,4,6-tetra-*O*-acetyl-1-thio-α-D-mannopyranoside[25,26]

α-D-Mannose pentaacetate (781 mg, 2.0 mmol) was dissolved in 20 mL anhydrous CH_2Cl_2. $BF_3 \cdot Et_2O$ (568 mg, 4.0 mmol) and 304 mg of thioacetic acid (4.0 mmol) were added to the stirred reaction mixture. The reaction mixture was stirred for 18 h under argon atmosphere. Thereafter, CH_2Cl_2 (200 mL) was added and the mixture was extracted with saturated aq. $NaHCO_3$ (200 mL). The organic phase was dried over Na_2SO_4, filtered and concentrated. Column chromatography (hexane/ethyl acetate, 6:4) gave the desired pentacetylated thiomannose. NMR was in good agreement with the reported literature data.[27]

Yield: 48%; ^{1}H NMR ($CDCl_3$): 5.95 (1H, s, H-1), 5.32–5.37 (2H, m, H-2, H-4), 5.10 (1H, dd, $J_{2,3} = 2.8$ Hz, $J_{3,4} = 10.1$ Hz, H-3), 4.29 (1H, dd, $J_{5,6'} = 4.8$ Hz, $J_{6,6'} = 12.6$ Hz, H-6'), 4.08 (1H, dd, $J_{5,6} = 2.5$ Hz, $J_{6,6'} = 12.6$ Hz, H-6), 2.44 (3H, s, S(O)CH_3), 3.91–3.96 (1H, m, H-5), 2.20, 2.09, 2.05, 2.00, (12H, 4 s, 4 COCH_3). FT-IR (ν): 2971, 2935 (C–H), 1750 [-(C = O) –O], 1714 [-(C = O) –S-], 753 cm^{-1} [-(S–OR)].

2.7.2. Deacetylation 1-*S*-Acetyl-2,3,4,6-tetra-*O*-acetyl-1-thio-α-D-mannopyranoside[27]

The titled compound (0.19 g, 0.5 mmol) and potassium methoxide (33 mg, 0.5 mmol) were mixed with 3 mL methanol and stirred for overnight. Afterwards, thin layer chromatography (TLC) (hexane/ethyl acetate, 1:1) indicated the formation of a single product (R_f 0.0, TLC plate was stained with vanillin and followed by strong heating using heat gun for better viewing). Ion exchange resin (DOWEX 50WX8-200) was added portionwise until the solution was neutralised, at which point the reaction mixture was concentrated in vacuo to yield the corresponding thiomannose. NMR was in good agreement with the reported literature data.[27]

Yield: 80%; ^{1}H NMR (CD_3OD): 5.51 (1H, d, $J_{1,2} = 1.6$ Hz, H-1) 5.07 (1H, d, H-1 of bis(thiomannose), 4.05 (1H, b, H-3), 3.92 (1H, b, H-2), 3.69–3.85 (3H, m, H-5, H-6, H-6'), 3.65 (1H, dd, $J_{3,4}$= 9.5 Hz, $J_{3,4}$= 9.7 Hz, H-4), ES-MS: *m/z* 195 (M–H$^+$, 100%). (HRMS (ES-) Calcd. for $C_6H_{11}O_5S$ (M–H$^+$) 195.0. Found: 195.0). FT-IR (ν): 3309 (O-H), 2983 (C-H), 2555 cm^{-1} [-S-H].

2.8. Michael Type Addition Between Acrylated PGMMA and 1-Thio-α-D-mannopyranose

1-Thio-α-D-mannopyranose (21/41/65 mg, 0.11/0.21/0.33 mmol, 1.5 times of acryloyl group) and 57/109/173 mg of TPP (0.22/0.42/0.66 mmol) were dissolved in 1 mL DMF and 1 mL methylene chloride, respectively. Then, the two solutions were mixed together and stirred for 10 min to reduce any disulfides generated from thiomannose. The thiomannose solution was added to the 13, 25 and 42 mol% acrylated PGMMA aqueous solution (100 mg polymer in 5 mL phosphate buffer, pH 7.4) and pH was adjusted to 7.8 using 1 M NaOH. After 15 min, methylene chloride was evaporated using rotary evaporator and subsequently the precipitate was removed by filtration. Finally, the filtered solution was further purified by dialysis using regenerated cellulose tubing (MWCO = 1 kDa) for 3 d and the polymers were isolated by freeze drying. Yield: 65%. All samples were characterised by ^{1}H NMR in D_2O. The disappearance of peaks at $\delta = 5.6$–6.6 ppm, which correspond to the protons of the acrylate group, indicated a quantitative conjugation of mannose. Furthermore, the peak intensity of the anomeric proton of thiomannose ($\delta = 5.4$ ppm) as well as the intensity of the protons at $\delta = 2.8$–3.2 ppm (4H, -S–CH_2–CH_2–CO–O-PGMMA) were compared to the CH_3 protons of the main polymer chain ($\delta = 0.80$–1.20 ppm, –CH_2C(CH_3)–) to calculate the degree of mannosylation (values calculated for the three polymers: 12, 24 and 40 mol% mannose/mol monomeric unit). Nuclear Overhauser enhancement (NOE) ^{1}H NMR was also performed to confirm the presence of a covalent bond between mannose and PGMMA (see Supporting Information).

2.9. Click Reaction Between Alkyne Terminated PGMMA and Azide-containing Molecules

11-ATA was firstly used as model azide compound to study the efficiency of the click conjugation with propargyl PGMMAs. Alkyne terminated PGMMA (0.1 g, 0.121 mmol -C≡CH) was weighed in an 8 mL glass vial. 11-ATA (5.3 mg, i.e., 1 equivalent of azide groups relative to -C≡CH) and DMF (1 mL) were added to the weighed PGMMA. The reaction mixture was purged with Argon for 5 min. Then, the ligand hexamethyl-triethylene tetraamine (5.6 mg) and catalyst CuBr (3.5 mg), i.e., 1 equiv. relative to -C≡CH, were added to the reaction mixture. The reaction was allowed to proceed at room temperature overnight. Afterwards, the reaction mixture was diluted with 10 mL of pure water and dialysed using regenerated cellulose tubing (MWCO =1 kDa) for 3 d, and freeze dried. Yield: 65%.

Compared with unreacted polymers, ^{1}H NMR (D_2O) spectrum of the product presented a new peak at 8.1 ppm, which corresponds to triazole methylene proton (Supporting Information, Figure S3). In ordert to evaluate the conversion of the click reaction, the product and pure PGMMA were hydrolyzed with 8 wt% NaOD (in D_2O) at room temperature for 1 h and analyzed by ^{1}H NMR. Hydrolyzed PGMMA clearly showed the peak at 4.18 ppm, which corresponds to propargyl alcohol (CH≡C–CH_2–OH). The disappearance of the same peak in hydrolyzed click-PGMMA product confirmed a conversion above 90% (Supporting Information, Figure S4).

The fluorophore Azide-MS673 was conjugated with propargyl PGMMAs following the same procedure as described above for 11-ATA. After freeze drying, ^{1}H NMR confirmed the presence of triazole methylene proton ($\delta = 8.1$ ppm). Fluorescence was confirmed at $\lambda_{em} = 673$ nm ($\lambda_{ex} = 542$ nm) in ethanol.

2.10. Production of BMDCs

BMDCs were prepared from bone marrow cells from C57Bl/6J mice, grown in the presence of 40 ng mL^{-1} of granulocyte-macrophage colony-stimulating factor (GM-CSF), according to a previously established method.[28] On day 6 of development, BMDCs were harvested, washed and re-suspended in complete RPMI-1640 media (RPMI-1640 (Gibco), 10% heat-inactivated foetal bovine serum, 5×10^{-5} M L-glutamine, 100 U mL^{-1} penicillin, 100 U mL^{-1} streptomycin, 5×10^{-6} M 2-mercapto-ethanol), and supplemented with 40 ng mL^{-1} GM-CSF. PGMMA and mannosylated PGMMA

were dissolved in Hank's Buffered Salt Solution (HBSS, Gibco), and filtered though a 0.22 μm syringe filter. Heat-inactivation of PGMMAs was by incubation at 95 °C for 10 min.

2.11. Cytotoxicity Tests

Cell viability was measured by a colorimetric assay based on the cleavage of the tetrazolium salt WST-1 by mitochondrial dehydrogenases, according to the manufacturer instructions (Cell Proliferation Reagent WST-1, Roche Applied Science). Cells in culture media were seeded and incubated in a 96 well plate at 37 °C in a humidified atmosphere of 5% CO_2 at a density of 8000 cells per well. After 24 h, the culture medium was replaced with a solution of fresh medium, containing varying concentrations of the PGMMA polymers, which were previously filtered through a sterile 0.22 μm filter. After 24 h, the incubation medium was removed, the cells were rinsed twice with phosphate-buffered saline (PBS) at pH 7.4, and their viability was analysed in triplicates. Data were normalised by the protein content of cells in each well, which was determined by bicinchoninic acid (BCA) protein determination assay (QuantiPro BCA assay kit, Sigma, Gillingham). The relative cell viability (%) was calculated as the ratio between the viability of cells incubated with the polymers and the control (i.e., viability of cells incubated solely with culture medium).

2.12. BMDC Stimulation

BMDC (5×10^5 cells mL^{-1}) were treated with increasing doses (0–1000 μg mL^{-1}) of mannosylated PGMMAs, heat-inactivated PGMMAs, as well as mannan. Ethylenediaminetetraacetic acid (EDTA, 5×10^{-3} M) was added to some samples to inhibit calcium-dependent mannose receptors.[29,30] Control BMDC received HBSS buffer alone. Some samples were supplemented with 1% non-heat-inactivated fetal bovine serum (FBS), as a source of active complement components. Supernatants were collected for detection of secreted cytokines and stored frozen at −80 °C. BMDC were examined for maturation by surface marker expression, by fluorescently-conjugate antibody staining, followed by flow cytometry (FACSarray, BD Biosciences).

2.13. Enzyme-linked Immunosorbent Assay (ELISA) of Cytokines

ELISA plates (Nunc) were coated with capture antibodies specific TNFα (100 ng per well), following wash and blocking with 2% bovine serum albumin (BSA)/PBS, and supernatant samples were added and the plates incubated overnight at 4 °C. Plates were washed, and bound cytokine detected using biotinylated antibodies specific for TNFα, and avidin-horseradish peroxidase (HRP). Final color development was performed using 1 mg mL^{-1} ortho-phenylene-diamine (OPD) in citrate buffer. Absorbance of samples at 450 nm was measured with a plate reader spectrophotometer (Dynatech) and a recombinant cytokine standard curve was derived to calculate the cytokine concentration in the samples. Data were normalised by the protein content of cells in each well, determined by BCA protein determination assay.

2.14. Flow Cytometry

For detection of BMDC surface marker upregulation, stimulated cells were washed with FACS buffer (PBS +2% FBS +0.02% NaN_3), and then stained with 100 ng of the following fluorescently conjugated antibodies: anti-CD40-APC, anti-CD11c-biotin and streptavidin-PE-Cy7, for 30 min at 4 °C. Following staining, cells were washed with FACS buffer, and fixed with neutral buffered formalin (Sigma), and the fluorescent staining measured using a FACS array flow cytometer (BD Biosciences). Fluorescence data was analysed using FlowJo software (TreeStar), and the percentage of CD11c-positive BMDC displaying positive CD40 surface expression was plotted.

2.15. Polymer Uptake

The amount of uptaken PGMMAs conjugated with Azide-MS673 (mannose content 0%-40%) was assessed upon 1–4 h incubation of BMDC cultured on sterile microscope coverslips with suspensions of fluorescently labelled polymers at concentration of 0–125 μg mL^{-1}. 5×10^{-5} M of EDTA was added to some samples to inhibit mannose receptors. After incubation, the medium was carefully removed and the cells were washed with ice-cold PBS and fixed with 4% paraformaldehyde (PFA) in PBS for 30 min at room temperature. The cells were then incubated with 4',6-diamidino-2-phenylindole (DAPI; 5 mg mL^{-1}) in PBS for 1 h prior imaging. The intracellular localization of fluorescent PGMMAs was examined via fluorescent microscopy (Leica DMI 6000 B, Leica Microsystem, UK). The extent of fluorescent staining was measured under the same conditions, except that cells were left un-fixed and subjected to flow cytometry using a FACS array flow cytometer (BD Biosciences) to calculate the % of MS673 positive cells.

2.16. Statistical Analysis

The unpaired Student t test, assuming equal variances, was used to determine the statistical significance of the difference in cytokine expression. Differences with p-values less than 0.05 were considered significant.

3. Results and Discussion

3.1. Synthesis of Functional PGMMAs

ATRP of glycerol monomethacrylate was carried out in methanol under facile conditions at room temperature, using Cu(I)Cl copper catalyst and bpy as ligand, according to protocols previously reported in literature.[19] PgBiB was used to allow a "click" reaction at one of the chain ends.[24,31,32] Although PgBiB has been frequently used as ATRP initiator,[33,34] in some works the alkyne functionality was protected with a trimethylsilyl group in order to circumvent complexation with the copper catalyst during polymerization,[35] and particularly in methanol.[36] In this case, PGMMAs at different molecular weight (with a DP

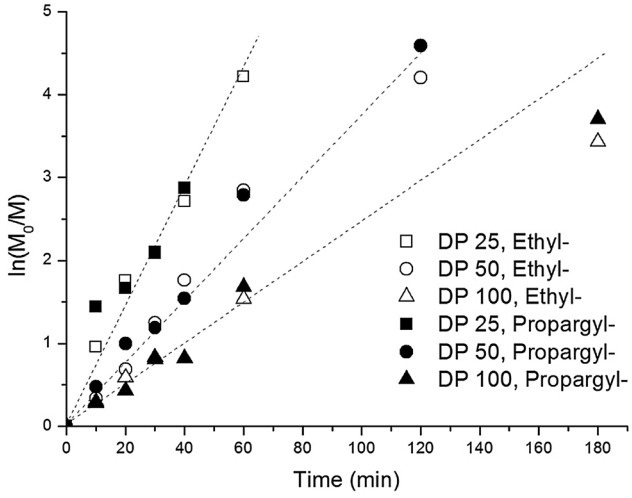

Figure 1. Kinetics of monomer consumption in the ATRP of GMMA as a function of monomer/initiator ratio (corresponding to degrees of polymerisation (DP) = 25, 50, and 100) and type of initiator (ethyl 2-bromoisobutyrate (EBiB), propargyl 2-bromoisobutyrate (PgBiB)).

varying from 25 to 100), were obtained without need of initiator protection/deprotection steps, and no sign of hydrolysis and/or transesterification could be highlighted[37] (see Supporting Information, Figure S1). Semilogarithmic plots of monomer concentration versus time (Figure 1) showed linearity up to high conversions, indicating first-order kinetics with constant concentration of active centres during polymerisation, both with the commercial EBiB initiator as well as with PgBiB initiator.

The relatively high polydispersity index measured for these polymers (1.30 for a DP = 50, Table 1) is in agreement with previous results regarding ATRP of GMMA carried out under similar conditions[19].

For the remainder of the study we focused on a PGMMA of $\overline{M}_n \approx 5$ kDa, corresponding to a DP = 25, which still bears a relatively high number of –OH groups available for conjugation, but likely provides rather limited steric hindrance to the terminal propargyl group, and whose limited size should allow for an eventual renal excretion, thus limiting the risk of a long-term permanence in an organism. This polymer was acrylated by a simple esterification with acryloyl chloride in DMF and triethylamine, in presence of BHT as radical inhibitor. Depending on acryloyl chloride/-OH molar ratios, PGMMAs at different degrees of acrylation were obtained. These polymers maintained a good solubility in water up to a molar ratio of 40% acrylate per monomeric unit. The extent of the acrylation was expressed as molar ratio acrylate/monomeric unit, thus assuming, for the sake of simplicity, that each acrylate is grafted on a different monomeric unit and that the conversion of a diol group of a GMMA unit into a diacrylate is statistically and sterically unfavored.

The Michael-type addition of 1-thio-α-D-mannopyranose was obtained at room temperature, with thiomannose and polymer dispersed in a mixture of DMF and phosphate buffer at pH 7.4–7.8. In order to reduce disulfides possibly formed from thiomannose, a solution of TPP in dichloromethane was also added to the mixture. Once the reaction was completed, the low boiling solvent was removed by rotary evaporation, and the precipitated TPP was easily removed by filtration. This method avoided side reactions and purification difficulties often encountered with the use of water-soluble tris(2-carboxyethyl)phosphine hydrochloride (TCEP) as disulfide reducing agent in Michael-type addition protocols.[38] Following dialysis and freeze drying, the mannosylated PGMMAs were characterised by ^{1}H NMR in D_2O (Figure 2). The disappearance of the peak at 5.6–6.6 ppm, corresponding to acrylate group, indicates a quantitative conversion of the Michael type addition reaction. Peaks at $\delta = 5.4$ and 2.8–3.2 ppm correspond to anomeric proton of thiomannose and mannose-S–CH_2-CH_2-CO–O-PGMMA, respectively. By comparing the intensity of these peaks to that of CH_3- protons (0.80–1.20 ppm) of the

Table 1. Molecular weight and dispersity index of PGMMAs as a function of its degree of polymerization DP.

Polymer	Initiator	DP	$M_{n,th}$ [a)]	$\overline{M}_{n,NMR}$ [b)]	$\overline{M}_{n,GPC}$ [c)]	$\overline{M}_w/\overline{M}_n$
PGMMA-25	EBiB	25	4199	-	5259	1.28
PGMMA-50	EBiB	50	8204	-	6630	1.30
PGMMA-100	EBiB	100	16 213	-	9702	1.32
PGMMA-25	PgBiB	25	4209	5375	5325	1.26
PGMMA-50	PgBiB	50	8214	9458	7472	1.30
PGMMA-100	PgBiB	100	16 223	15 827	9086	1.32

[a)] $M_{n,th}$ is referred to the theoretical values of $\overline{M}_n$ determined by the molar ratio monomer/initiator used in ATRP. [b)] $\overline{M}_{n,NMR}$ was determined by ^{1}H-NMR; [c)] $\overline{M}_{n,GPC}$ and the polydispersity index $\overline{M}_w/\overline{M}_n$ were calculated from GPC.

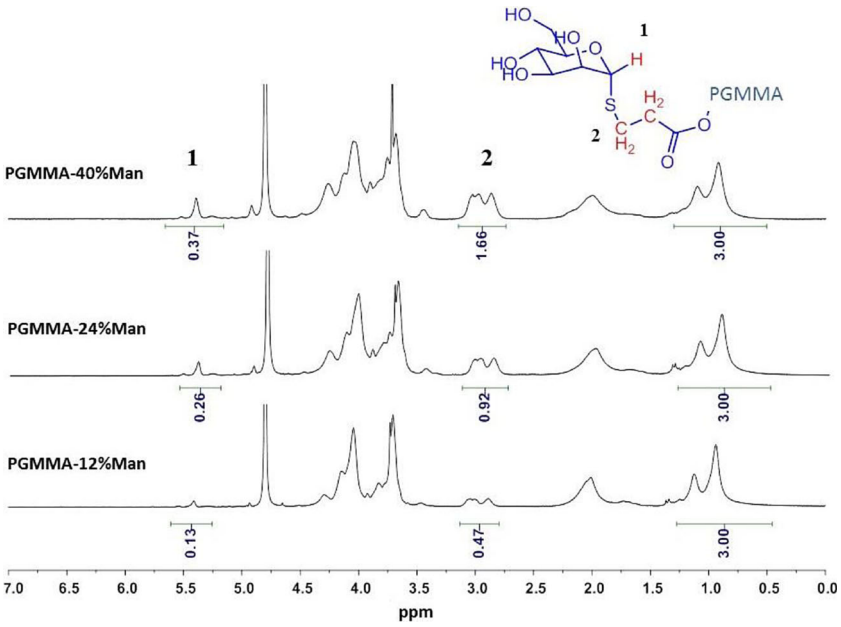

Figure 2. ^{1}H NMR (D_2O) spectra of 12, 24 and 40% mannosylated PGMMAs.

PGMMA backbone, the amount of mannose attached to the polymers was calculated to be 12, 24, and 40 mol% per mol of monomeric unit, indicating a complete conversion of the acrylate groups.

3.2. Dendritic Cell Viability and Stimulation in Vitro

Mannose linked poly(glycerol methacrylate)s (Man-PGMMAs) at different degree of mannosylation, including propargyl PGMMA without grafted mannose as control, were tested in vitro on murine BMDCs grown in cell culture, to assess their effect on cell viability and APC activation.

3.2.1. Cytotoxicity Tests

Cytotoxicity tests were performed through a colorimetric tetrazolium-based assay (WST-1 assay) on BMDCs in presence of PGMMA 0%, 24%, 40% mannose, respectively. All polymers confirmed a safe cytotoxic profile, showing unaltered cell viability for concentrations up to 1 mg mL^{-1} (Figure 3), i.e., within a concentration range compatible with the cytokine release tests.

3.2.2. BMDC Activation

The immune activity of the polymers was tested by monitoring cytokines released by BMDCs in vitro, as an effect of PGMMA composition and concentration in culture media.

Firstly, we focused on BMDC expression of tumor necrosis factor-alpha (TNFα), which plays a primary role in the regulation of immune cells. TNFα is generally involved in systemic inflammation and is a member of a group of cytokines that stimulate the acute phase reaction. Apart from its role in mediating innate immune responses, TNFα is also involved in the maturation of DC after viral challenge, highlighting the importance of this innate cytokine in activating adaptive immunity.[39]

Expression of TNFα was assessed in the presence of PGMMA having different amount of grafted mannose. The effect of polymer concentration and mannose content on TNFα release is shown in Figure 4. Heat-inactivated polymers (i.e., PGMMAs incubated at 95 °C for 10 min to cleave the mannose groups by rapid hydrolysis of the thioether-ester bond[40])) were also tested for comparison. The effects of serum complement components was also assessed by supplementing the cells with 1% non-heat-inactivated FBS. A clear trend of response with increasing amount of mannose groups was noticed (Figure 4). This confirmed that the amount of side-chain mannose influences BMDC activation. The non-linear trend of cytokine expression with concentration, indicated a possible polymer concentration threshold (between 0–100 μg mL^{-1}) below which cells cannot be activated. A clear effect of complement proteins was also noticed, as the response was much higher when the tests were performed in the presence of non-heat-inactivated serum. Pre-heated polymers were mostly unable to trigger TNFα expression, thus confirming that mannose has to be

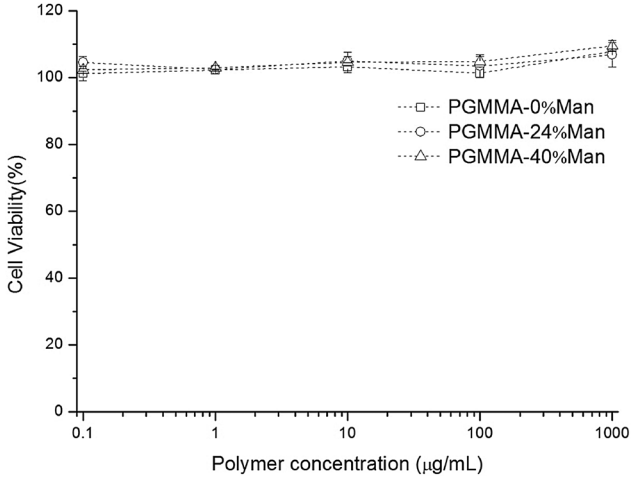

Figure 3. Cell viability measured via the WST-1 assay and normalized per mg of protein, using untreated cells as negative control.

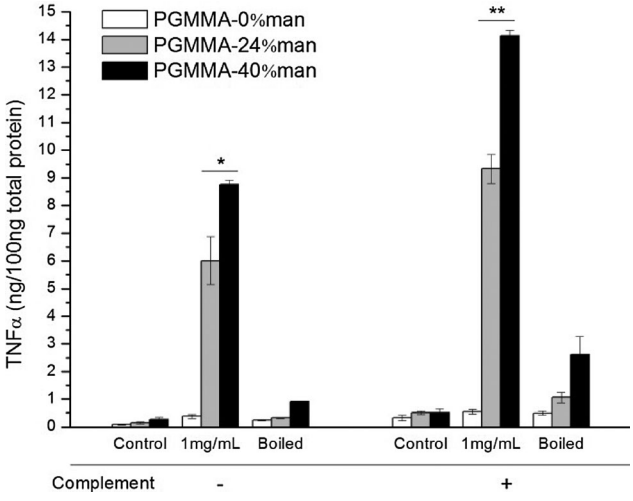

Figure 4. TNF-α expression (ELISA) by BMDC in presence of mannosylated PGMMAs, with and without pre-heat-inactivation (Boiled), and +/– active serum complement components in culture medium. (* $p < 0.05$, ** $p < 0.01$).

grafted to the polymeric backbone to induce the BMDC response.

We then compared the activity of Man-PGMMAs to mannan, i.e., a commercial yeast-derived polymannose (Figure 5A,B). While this material stimulated a high TNFα expression without a gradual response to concentration (mannan at any concentration in the 100–1000 μg mL^{-1} range (Figure 5A), corresponding to ca. 0.6–6 mM range (Figure 5B) provided a substantially constant TNFα release), PGMMAs showed a milder immune activation and a more pronounced concentration dependence of cytokine expression. In particular, Figure 5B shows how mannan (see point at a mannose molar concentration of 0.56 mM) stimulated a 2–3 fold increase of TNFα expression compared with PGMMAs at similar mannose concentrations (0.2–2 mM range).

In presence of EDTA, i.e., a mannose-receptor inhibitor (mannose binding is known to be Ca^{++}-dependent and EDTA acts as a Ca^{++} sequestrant),[29,30] all mannose-containing polymers lost their ability to stimulate cytokine expression, thus confirming the role of mannose in activating dendritic cells through a calcium-dependent mannose-receptor binding.

The expression of the membrane protein CD40 was also investigated to characterise the activation of BMDCs. In fact, CD40 has been shown to stimulate DC maturation and may work together with TNFα for efficient immune activation.[39,41,42] CD40 expression followed a similar trend as the expression of TNFα (Figure 6). The percentage of CD40-positive BMDC, quantified by flow cytometry, was dependent on PGMMA concentration and mannosylation extent, and it was more pronounced when BMDCs were stimulated by mannan instead of PGMMAs.

3.2.3. Polymer Uptake

The advantage of having a 'clickable' alkyne as terminal functional group in PGMMA-based polymers was exploited by in vitro cellular uptake studies. The azide-containing fluorophore Azide-MS673 was efficiently linked to mannosylated Pg-PGMMA through Huisgen cycloaddition at room temperature to obtain fluorescently-labelled polymers. Preliminary uptake studies were carried out with fluorecently labelled PGMMAs incubated with BMDCs.

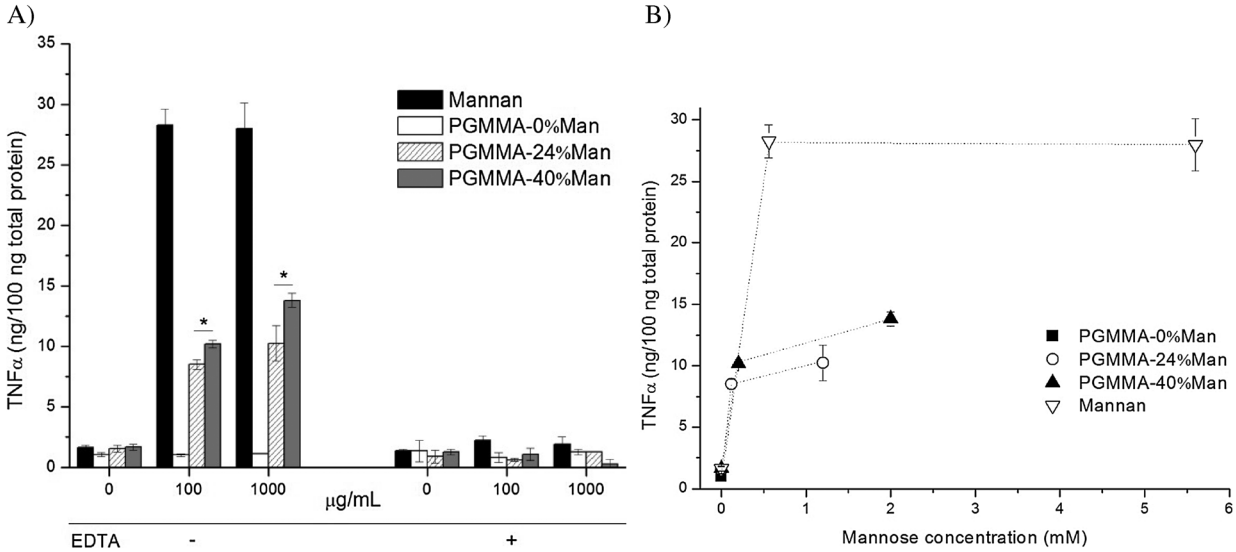

Figure 5. A) TNF-α expression by BMDC in presence of mannan, mannosylated PGMMAs, +/– EDTA in medium (polymer concentrations in μg mL^{-1}) (* $p < 0.05$, ** $p < 0.01$). B) TNF-α expression ((– EDTA) data as reported in A) plotted as a function of the molar concentration of mannose.

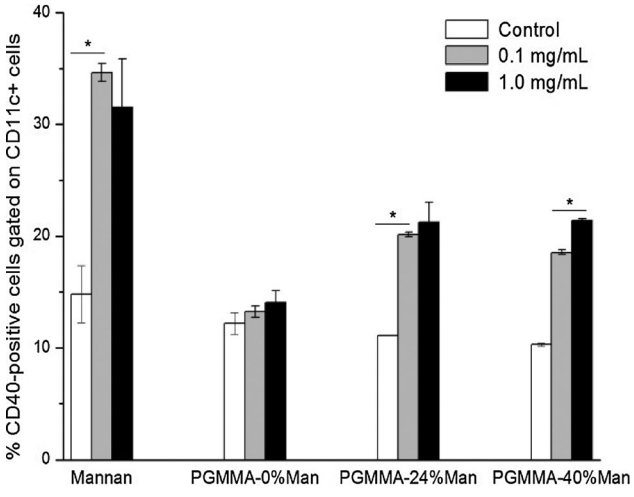

Figure 6. CD40 expression (%CD40-positive cells gated on CD11c+ cells by FACS analysis) by BMDC in presence of mannan and mannosylated PGMMAs (* $p < 0.05$).

Optical microscopy showed an efficient internalisation of PGMMAs, highlighted by an intracellular fluorescence localised in punctiform vesicles, which may indicate a possible lysosomal internalisation of the polymers (Figure 7). This effect was observed with all polymers tested. Quantitative flow cytometry analysis was used to determine the fraction of cells containing fluorescent polymer within the first hour of incubation of PGMMAs with BMDC. The results showed that PGMMAs with grafted mannose were more efficiently co-localised than the non-mannosylated polymer, although a clear effect of mannose content (24% vs 40%) on BMDC staining was not appreciated. However, polymer-cell interaction uptake was sensibly reduced by the presence of EDTA. As discussed in BMDC activation, EDTA is a calcium-sequestrant agent, and when this inhibitor is added to the cell medium it removes the free calcium that mannose receptors (MR) require for carbohydrate binding.[22,43] It has been reported that without MR binding, mannose-containing macromolecules could not be efficiently internalized.[44]

These results suggested that mannose was actively involved with the internalisation mechanism through a mannose-receptor mediated endocytosis.

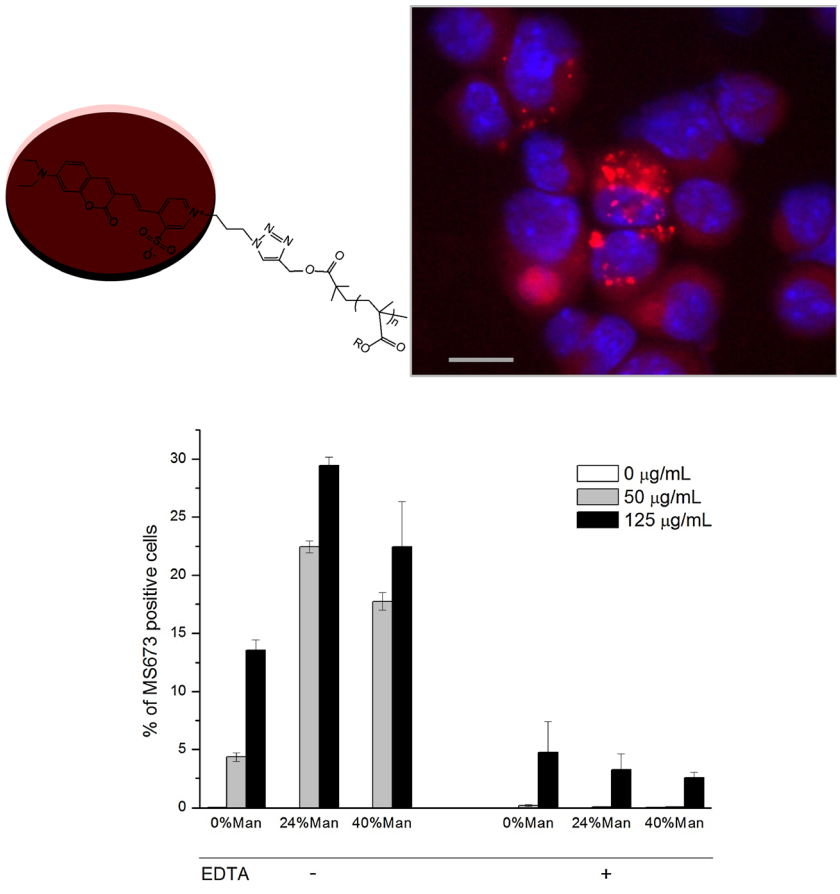

Figure 7. Top. The fluorophore Azide-MS673 was linked to the PGMMA by azide-alkyne click reaction. The resulting fluorescent polymer (PGMMA-40%Man, 50 μg mL^{-1}) was incubated with BMDC and observed as intracellular fluorescence (image at 4 h incubation time, bar 10 μm). *Bottom.* Effect of % mannosylation, polymer concentration and presence of EDTA on fraction of BMDC containing fluorescent polymer (% of MS673 positive cells) measured by flow cytometry after 1 h incubation.

4. Conclusion

A versatile synthetic approach based on controlled/living polymerisation and click chemistry techniques was developed to produce immunoactive polymeric templates with highly controlled molecular weight and functionality. Propargyl-terminated PGMMAs were successfully synthesized and modified with dangling acrylate groups at different degree of functionalisation. Acrylates were then able to react with thiolated mannose through Michael-type addition. The propargyl terminal group was modified independently with azide end-capping groups and utilized to graft the macromolecules to a fluorescent dye. Preliminary in vitro tests confirmed a safe cytotoxicity profile, as well as the immunostimulatory functions of the polymers. Mannose linked PGMMAs were able to stimulate cytokine production and membrane protein expression in BMDC. The extent of cell activation and uptake was dependent on the mannose content, is sensitive to calcium, and was

enhanced by serum complement proteins, consistent with a mechanism of mannose-mediated complement activation and/or binding to mannose receptors on the cell membrane.

This approach paves the way for a rational design and synthesis of new immunoactive macromolecules, which can display a tuneable amount of cell-activating groups of different type, thus creating extensive combinations of saccharides, hydroxyl groups, toll-like receptor ligands, all assembled with the same "click" technique. This synthetic strategy may also allow a very simple polymer conjugation with (cysteine containing) antigen peptides, with the possibility of generating materials that act as adjuvants as well as vaccines with programmed antigen uptake and presentation. Moreover, the polymeric material may be efficiently linked to proteins, other macromolecules or nanoparticles by alkyne-azide click reactions, thus generating nanomaterials for tailored delivery strategies.

Acknowledgements: The authors thank the Engineering and Physical Sciences Research Council (EPSRC) in UK for funding (Grant EP/H027092/1).

Received: March 25, 2014; Revised: July 1, 2014; Published online: August 18, 2014

[1] R. Duncan, M. J. Vicent, *Adv. Drug Delivery Rev.* **2013**, *65*, 60.
[2] Y. Zhang, H. F. Chan, K. W. Leong, *Adv. Drug Delivery Rev.* **2013**, *65*, 104.
[3] M. D. Howard, M. Jay, T. D. Dziublal, X. L. Lu, *J. Biomed. Nanotechnol.* **2008**, *4*, 133.
[4] J. A. Hubbell, S. N. Thomas, M. A. Swartz, *Nature* **2009**, *462*, 449.
[5] D. M. Smith, J. K. Simon, J. R. Baker, *Jr., Nat. Rev. Immunol.* **2013**, *13*, 592.
[6] T. D. Nandedkar, *J. Biosci.* **2009**, *34*, 995.
[7] Y. Perrie, A. R. Mohammed, D. J. Kirby, S. E. McNeil, V. W. Bramwell, *Int. J. Pharm.* **2008**, *364*, 272.
[8] S. L. Demento, A. L. Siefert, A. Bandyopadhyay, F. A. Sharp, T. M. Fahmy, *Trends Biotechnol.* **2011**, *29*, 294.
[9] D. J. Irvine, M. A. Swartz, G. L. Szeto, *Nat. Mater.* **2013**, *12*, 978.
[10] N. Petrovsky, J. C. Aguilar, *Immunol. Cell Biol.* **2004**, *82*, 488.
[11] Z. Wu, Y. Du, H. Xue, Y. Wu, B. Zhou, *Neurobiol. Aging* **2012**, 33.
[12] M. A. Swartz, J. A. Hubbell, S. T. Reddy, *Semin. Immunol.* **2008**, *20*, 147.
[13] A. Gamvrellis, D. Leong, J. C. Hanley, S. D. Xiang, P. Mottram, M. Plebanski, *Immunol. Cell Biol.* **2004**, *82*, 506.
[14] G. Robert-Nicoud, R. Evans, C.-D. Vo, C. J. Cadman, N. Tirelli, *Polym. Chem.* **2013**, *4*, 3458.
[15] R. Haigh, S. Rimmer, N. J. Fullwood, *Biomaterials* **2000**, *21*, 735.
[16] S. Rimmer, C. Johnson, B. Zhao, J. Collier, L. Gilmore, S. Sabnis, P. Wyman, C. Sammon, N. J. Fullwood, S. MacNeil, *Biomaterials* **2007**, *28*, 5319.
[17] E. Patrucco, S. Ouasti, C. D. Vo, P. De Leonardis, A. Pollicino, S. P. Armes, M. Scandola, N. Tirelli, *Biomacromolecules* **2009**, *10*, 3130.
[18] K. Mequanint, A. Patel, D. Bezuidenhout, *Biomacromolecules* **2006**, *7*, 883.
[19] M. Save, J. V. M. Weaver, S. P. Armes, P. McKenna, *Macromolecules* **2002**, *35*, 1152.
[20] P. D. Topham, N. Sandon, E. S. Read, J. Madsen, A. J. Ryan, S. P. Armes, *Macromolecules* **2008**, *41*, 9542.
[21] C. Giacomelli, V. Schmidt, R. Borsali, *Macromolecules* **2007**, *40*, 2148.
[22] P. R. Taylor, S. Gordon, L. Martinez-Pomares, *Trends Immunol.* **2005**, *26*, 104.
[23] S. Burgdorf, A. Kautz, V. Bohnert, P. A. Knolle, C. Kurts, *Science* **2007**, *316*, 612.
[24] N. V. Tsarevsky, B. S. Sumerlin, K. Matyjaszewski, *Macromolecules* **2005**, *38*, 3558.
[25] I. Hamachi, T. Nagase, S. Shinkai, *J. Am. Chem. Soc.* **2000**, *122*, 12065.
[26] B. D. Johnston, B. M. Pinto, *J. Org. Chem.* **2000**, *65*, 4607.
[27] G. J. L. Bernardes, D. P. Gamblin, B. G. Davis, *Angew. Chem. Int. Ed.* **2006**, *45*, 4007.
[28] M. B. Lutz, N. Kukutsch, A. L. J. Ogilvie, S. Rossner, F. Koch, N. Romani, G. Schuler, *J. Immunol. Methods* **1999**, *223*, 77.
[29] D. G. Nguyen, J. E. K. Hildreth, *Eur. J. Immunol.* **2003**, *33*, 483.
[30] G. D. Chazenbalk, P. N. Pichurin, J. Guo, B. Rapoport, S. M. McLachlan, *Clin. Exp. Immunol.* **2005**, *139*, 216.
[31] B. A. Laurent, S. M. Grayson, *J. Am. Chem. Soc.* **2006**, *128*, 4238.
[32] Q. H. Zhou, J. K. Zheng, Z. H. Shen, X. H. Fan, X. F. Chen, Q. F. Zhou, *Macromolecules* **2010**, *43*, 5637.
[33] W. Van Camp, V. Germonpre, L. Mespouille, P. Dubois, E. J. Goethals, F. E. Du Prez, *React. Funct. Polym.* **2007**, *67*, 1168.
[34] W. Agut, D. Taton, S. Lecommandoux, *Macromolecules* **2007**, *40*, 5653.
[35] J. A. Opsteen, J. C. M. van Hest, *Chem. Commun.* **2005**, 57.
[36] X. S. Fan, G. W. Wang, J. L. Huang, *J. Polym. Sci., Part A: Polym. Chem.* **2011**, *49*, 1361.
[37] L. S. Connell, J. R. Jones, J. V. M. Weaver, *Polym. Chem.* **2012**, *3*, 2735.
[38] G.-Z. Li, R. K. Randev, A. H. Soeriyadi, G. Rees, C. Boyer, Z. Tong, T. P. Davis, C. R. Becer, D. M. Haddleton, *Polym. Chem.* **2010**, *1*, 1196.
[39] J. M. Trevejo, M. W. Marino, N. Philpott, R. Josien, E. C. Richards, K. B. Elkon, E. Falck-Pedersen, *Proc. Natl. Acad. Sci. USA* **2001**, *98*, 12162.
[40] A. E. Rydholm, K. S. Anseth, C. N. Bowman, *Acta Biomater.* **2007**, *3*, 449.
[41] H. Jonuleit, J. Knop, A. H. Enk, *Arch. Dermatol. Res.* **1996**, *289*, 1.
[42] C. Caux, C. Massacrier, B. Vanbervliet, B. Dubois, C. Vankooten, I. Durand, J. Banchereau, *J. Exp. Med.* **1994**, *180*, 1263.
[43] N. P. Mullin, P. G. Hitchen, M. E. Taylor, *J. Biol. Chem.* **1997**, *272*, 5668.
[44] F. Sallusto, M. Cella, C. Danieli, A. Lanzavecchia, *J. Exp. Med.* **1995**, *182*, 389.